Computing Handedness: Quantized and Superposed Switch and Dynamic Memory of Helical Polysilylene

Michiya Fujiki,*,†,§ Julian R. Koe,†,§ Masao Motonaga,§ Hiroshi Nakashima,†,§ Ken Terao,§ and Akio Teramoto‡,§

Contribution from the NTT Basic Research Laboratories, 3-1 Wakamiya, Morinosato, Atsugi, Kanagawa 243-0198, Japan, Ritsumeikan University, Research Organization of Science and Engineering, 1-1-1 Nojihigashi, Kusatsu, Shiga 525-8577, Japan, and CREST-JST (Japan Science and Technology Corporation), 4-1-8 Honcho, Kawaguchi, Saitama 332-0012, Japan

Received July 18, 2000

Abstract: Two new conjugating helical polymers comprising a rodlike silicon backbone and enantiopure chiral pendants, poly{(*R*)-3,7-dimethyloctyl-(*S*)-3-methylpentylsilylene} (**PS-1**) and its diastereomeric poly{(*S*)-3,7-dimethyloctyl-(*S*)-3-methylpentylsilylene} (**PS-2**), were prepared. Molecular mechanics calculations of **PS-1** and **PS-2** model oligomers indicated a double well potential energy curve corresponding to almost enantiomeric helices with dihedral angles of 150−160° (*P*-motif, global minimum) and 200−210° (*M*-motif), regardless of their tacticity. Experimentally, it was found that **PS-1** in dilute isooctane revealed switchable ambidextrous helicity on application of a thermal energy bias. Although **PS-1** featured three distinct switching regions, viz. "region 1, between −80 and −10 °C", "region 2, between −10 and +10 °C", and "region 3, between +10 °C and +80 °C", the switching properties were interpreted as the result of superposed *P*- and *M*-helicities, undergoing dynamic pseudo-racemization or oscillation. Oscillating helicity in region 2 was roughly estimated to be about 13 cm^{-1}. The superposed helicity in region 2 was critical since it afforded molecular recognition ability with a dynamic memory function that was highly susceptible to solvent molecular topology and volume fraction. This could lead to potential as a molecular information processor to serve as a gauge of chemical properties. On the other hand, **PS-2** could not switch its preferential screw-sense in the range of −80 to +80 °C. This may be related to greater differences the potential energy curve between *P*- and *M*-motifs.

1. Introduction

Designing and realizing miniature-scale computing devices are now challenging issues in molecular science and nanotechnology.[1] A chiral molecular switch and memory with a two-state "on−off" function, linked with molecular motions such as twist,[2] rotate,[3] fold,[4] shrink,[5] stack,[6] and shuttle,[7] may be a candidate as basic elements in such devices. Nevertheless, molecular-based elements remain problematic, due to difficulties in the wiring of these elements along with "memory" function, defined threshold, processing, and error correction. However, understanding and measuring the superposition of bi-stable quantum states ("a quantum bit" or "qubit") in nanosystems based on semiconductors and superconductors are current theoretical and experimental topics directed toward the development of quantum computing.[8] To overcome some problems in conventional digital computing, "quantum computing" using the controlled mixing of "on−off" states and "0−1" bits may provide a method to save much processing time and energy.[8]

† NTT Basic Research Laboratories.

‡ Ritsumeikan University.

§ CREST-JST.

(1) (a) Wilson, E. K. *Chem. Eng. News* **2000** (Nov. 6), 35−39. (b) Feynman, R. *Science* **1991**, *254*, 1300−1301. (c) Drexler, K. E. *Nanosystems: Molecular Machinery, Manufacturing and Computing*; Wiley: New York, 1992.

(2) (a) Bradbury, E. M.; Carpenter, B. G.; Goldman, H. *Biopolymers* **1968**, *6*, 837−850. (b) Pohl, F. M.; Jovin, T. M. *J. Mol. Biol*. **1972**, *67*, 375−396. (c) Toriumi, H.; Saso, N.; Yasumoto, Y.; Sasaki, S.; Uematsu, I. *Polym. J*. **1979**, *11*, 977−981. (d) Okamoto, Y.; Nakano T.; Ono, E.; Hatada K. *Chem. Lett.* **1991**, 525−528. (e) Maxein, G.; Zentel, R. *Macromolecules* **1995**, *28*, 8438−8440. (f) Bouman, M. M.; Meijer, E. W. *Adv. Mater*. **1995**, *7*, 385−387. (g) Agati G.; McDonagh, A. F. *J. Am. Chem. Soc*. **1995**, *117*, 4425−4426. (h) Mahadevan, S.; Palaniandavar, M. *Chem. Commun*. **1996**, 2547−2548. (i) Bidan G.; Guillerez S.; Sorokin V. *Adv. Mater*. **1996**, *8*, 157−160. (j) Watanabe, J.; Okamoto, S.; Satoh, K.; Sakajiri, K.; Furuya, H.; Abe, A. *Macromolecules* **1996**, *29*, 7084−7088. (k) Yamaguchi, T.; Uchida, K.; Irie, M. *J. Am. Chem. Soc*., **1997**, *119*, 6066−6071. (l) Yashima, E.; Maeda, K.; Okamoto, Y. *J. Am. Chem. Soc*. **1998**, *120*, 8895−8896. (m) Maeda, K.; Okamoto, Y. *Macromolecules* **1999**, *32*, 974−980. (n) Burnham, K. S.; Schuster, G. B. *J. Am. Chem. Soc*. **1999**, *121*, 10245−10246. (o) Mao, C.; Sun, W.; Shen, Z.; Seeman, N. D. *Nature* **1999**, *397*, 144−146. (p) Yashima, E.; Maeda, K.; Okamoto, Y. *Nature* **1999**, *399*, 449−451. (q) Li, J.; Schuster, G. B.; Cheon, K.-S.; Green, M. M.; Selinger, J. V. *J. Am. Chem. Soc*. **2000**, *122*, 2603−2612. (r) Cheon, K.-S.; Selinger, J. V.; Green, M. M. *Angew. Chem., Int. Ed.* **2000**, *39*, 1482−1485.

(3) (a) Koumura, N.; Zijistra, R. W.; van Delden, R. A.; Harada, N.; Feringa, B. L. *Nature* **1999**, *401*, 152−154. (b) Feringa, B. L.; Jager, W. F.; de Lange, B.; Meijer, E. W. *J. Am. Chem. Soc*. **1991**, *113*, 5468−5470 1991. (c) Kelly, T. R.; De Silva, H.; Silva, R. A. *Nature* **1999**, *397*, 150−152.

(4) (a) Schmieder, R.; Hübner, G.; Seel, C.; Vögtle, F. *Angew. Chem., Int. Ed*. **1999**, *38*, 3528−3530. (b) Bedard, T. C.; Moore, J. S. *J. Am. Chem. Soc*. **1995**, *117*, 10662−10671. (c) Nelson, J. C.; Saven, J. G.; Moore, J. S.; Wolynes, P. G. *Science* **1997**, *277*, 1793−1796. (d) Gin, M. S.; Yokozawa, T.; Prince, R. B.; Moore, J. S. *J. Am. Chem. Soc*. **1999**, *121*, 2643−2644.

(5) Zahn, S.; Canary, J. W., *Angew. Chem., Int. Ed*. **1998**, *37*, 305−307.

(6) Engelkamp, H.; Middelbeek, R.; Nolte, R. J. M. *Science* **1999**, *284*, 785−788.

(7) Murakami, H.; Kawabuchi, A.; Kotoo, K.; Kunitake, M.; Nakashima, N. *J. Am. Chem. Soc*. **1997**, *119*, 7605−7606.

(8) (a) Lloyd, S. *Sci. Am.* **1995**, *273(4)*, 140−145. (b) Gershenfeld, N.; Chuang, I. L. *Sci. Am*. **1998**, *278(6)*, 66−71. (c) Oosterkamp, T. H.; Fujisawa, T.; van der Wiel, W. G.; Ishibashi, K.; Hijman, R. V.; Tarucha, S.; Kouwenhoven, L. P. *Nature* **1999**, *395*, 873−876. (d) Nakamura, Y.; Pashkin, Y.-A.; Tsai, J. S. *Nature* **1999**, *398*, 786−788.

10.1021/ja0026509 CCC: $20.00
Published on Web 06/09/2001

Before these boom studies, although several quantum chemists[9] had already discussed quantum tunneling and oscillation, and the preparation and detection of superposed optical activity for a hypothetical chiral molecule with a double-well potential, they did not infer from their ideas the possibility of quantum computing based on a chiral molecule.

A stiff helical polysilylene, consisting of stretchable, rotatable silicon−silicon single bonds in a helical backbone bearing enantiopure chiral pendants[10,11] may be a potential candidate chiral molecule with which to test the idea of the superposition of *P* (plus, right-handed) and *M* (minus, left-handed) states and to construct a molecular processor susceptible to external physical and chemical stimuli. This is because the helical polysilylene has (a) essentially two conformational *P*- and *M*-states, but may show marked cooperative conformational change in response to external stimuli,[11a,b] similar to other stiff helical polymers,[13] (b) a unique, intense CD signal with matching near-UV absorption with narrow bandwidth of 4−8 nm, characteristic of its "one-dimensional exciton with discrete energy levels",[10] which allows the quantitative analysis of the chiroptical switching states and population of *P*- and *M*-states[10,11] using the physically clearer Kuhn's dissymmetry ratio $\{g_{abs} = \Delta\epsilon/\epsilon = 2(\epsilon_L - \epsilon_R)/(\epsilon_L + \epsilon_R)\}$, rather than $\Delta\epsilon$ and specific optical rotation ([α]), whose $\Delta\epsilon$ and ϵ are the CD and UV peak intensities, and ϵ_L and ϵ_R are the absorption intensities for left and right circular polarized light,[13] respectively, and (c) an almost insulating semiconducting state which may be rendered highly conducting by injection of electron or hole carriers into the backbone.[10e]

Previous stiff helical polysilylenes with enantiopure β-branched chiral and long *n*-alkyl pendants, however, adopt only a single-handed screw-sense helix (positive CD signal only) and are not susceptible to any external physical or chemical stimuli, due to severe restriction of twisting motions in their rigid structures.[10] Also, the recently reported helical polysilylenes which undergo inversion of preferential helicity are inadequate to test the validity of these ideas, due to their lower inversion temperatures of −20 °C.[11a,b]

With these problems in mind, two new stiff helical polysilylenes, poly{(*R*)-3,7-dimethyloctyl-(*S*)-3-methylpentylsilylene} (**PS-1**, Scheme 1) and poly{(*S*)-3,7-dimethyloctyl-(*S*)-3-methylpentylsilylene} (**PS-2**, Scheme 1), were prepared according to the standard Wurtz procedure described in the literature.[10d,11a] The former features *opposite* handedness in the γ-positions of different enantiopure chiral pendants, while the latter contains substituents with the *same* handedness.

Scheme 1. Chemical Structures of Poly[(*R*)-3,7-dimethyloctyl-(*S*)-3-methylpentylsilylene] (**PS-1**), Poly-[(*S*)-3,7-dimethyloctyl-(*S*)-3-methylpentylsilylene] (**PS-2**), Poly[(*S*)-3,7-dimethyloctyl-3-methylbutylsilylene] (**PS-3**), and Poly[(*S*)-3,7-dimethyloctyl-2-methylpropylsilylene] (**PS-4**)

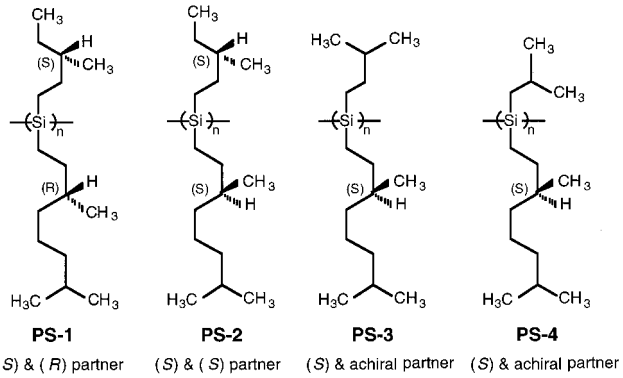

Here we report that the choice of handedness in the two chiral pendants definitively determines the inversion capability of the chiroptical properties associated with a preferential screw-sense: Only **PS-1** in dilute solution revealed switchable ambidextrous helicity on application of a thermal energy bias. Although **PS-1** in dilute isooctane features three distinct switching regions, viz. "between −80 and −10 °C", "between −10 and +10 °C", and "between +10 °C and +80 °C", these switching properties are interpreted as the result of the superposition of *P*- and *M*-states. The superposed helicity between −10 and +10 °C is of particular importance with respect to molecular recognition ability and dynamic memory function, since it is highly susceptible to solvent molecular topology and volume fraction.

2. Results and Discussion

2.1. Comparison of Polysilylenes with and without Helix−Helix Transitions. As shown in Figure 1a, the positive-signed CD spectrum of **PS-1** for high-molecular weight polymer with an extremum of 320 nm at −60 °C in isooctane is almost the inverse of the negative-signed CD spectrum with an extremum of 325 nm at +25 °C. This indicates that the helical conformations at the two temperatures are almost equivalent, except for the direction of their preferential helical screw-senses. The respective CD spectra, with matching UV absorption spectral profiles in the range of −80 to +80 °C, are consistent with the partial cancellation of positive and negative CD signals.[14] These are associated with an imbalance in the populations of pseudo-enantiomeric *P*- and *M*-motifs in the same chain with the same CD extrema.

Figure 1b shows that the $\Delta\epsilon$ value of **PS-1** changes with lowering temperature from ca. −4.3 at +80 °C, passes through a broad minimum of −6.5 around +20 °C, increases abruptly

(9) (a) Cina, J. A.; Harris, R. A. *Science* **1995**, *267*, 832−833. (b) Cina, J. A.; Harris, R. A., *J. Chem. Phys.* **1994**, *100*, 2531−2536. (c) Harris, R. A., *Chem. Phys. Lett.* **1994**, *223*, 250−254. (d) Quack, M. *Chem. Phys. Lett.* **1986**, *132*, 147−153. (e) Harris, R. A.; Stodolsky, L. *Phys. Lett.* **1978**, *78B*, 313−317. (f) Janoschek, R. In *Chirality*; Janoschek, R., Ed.; Springer: Berlin, 1992; Chapter 2. (g) Barron, L. D. In *New Developments in Molecular Chirality*; Mezey, P. G., Ed.; Kluwer-Academic: Dordrecht, The Netherlands, 1990; pp 34−37.

(10) (a) Fujiki, M. *J. Am. Chem. Soc.* **1994**, *116*, 6017−6018. (b) Fujiki, M. *Appl. Phys. Lett.* **1994**, *65*, 3251−3253. (c) Ebihara, K.; Koshihara, S−y.; Yoshimoto, M.; Maeda, T.; Ohnishi, T.; Koinuma, H.; Fujiki, M. *Jpn. J. Appl. Phys.* **1997**, *36*, L1211-L1213. (d) Fujiki, M.; Toyoda, S.; Yuan, C.-H.; Takigawa, H. *Chirality* **1998**, *10*, 667−675. (e) Ichikawa, T.; Yamada, Y.; Kumagai, J.; Fujiki, M. *Chem. Phys. Lett.* **1999**, *306*, 275−279. (f) Fujiki, M. *J. Am. Chem. Soc.* **1996**, *118*, 7424−7425. (g) Toyoda, S.; Fujiki, M.; Suzuki, H.; Matsumoto, N. *Solid State Commun.* **1997**, *103*, 87−89.

(11) (a) Fujiki, M. *J. Am. Chem. Soc.* **2000**, *122*, 3336−3343. (b) Koe, J. R.; Fujiki, M.; Motonaga, M.; Nakashima, H. *Chem. Commun.* **2000**, *2000*, 389−390. (c) Koe, J. R.; Fujiki, M.; Nakashima, H. *J. Am. Chem. Soc.* **1999**, *121*, 9734−9735.

(12) Schilling, F. C.; Lovinger, A. J.; Zeigler, J. M.; Davis, D. D.; Bovey, F. A. *Macromolecules* **1989**, *22*, 3055−3063.

(13) (a) Green, M. M.; Park, J. W.; Sato, T.; Teramoto, A.; Lifson, S.; Selinger, R. L. B.; Selinger, J. V. *Angew. Chem., Int. Ed.* **1999**, *38*, 3138−3154. (b) Teramoto, A. *Rep. Prog. Polym. Phys. Jpn.* **1998**, *41*, 25−65. (c) Khatri, C. A.; Pavlova, Y.; Green, M. M.; Morawetz, H. *J. Am. Chem. Soc.* **1997**, *119*, 6991−6995. (d) Green, M. M.; Khatri, C. A.; Peterson, N. C. *J. Am. Chem. Soc.* **1993**, *115*, 4941−4942. (e) Cheon, K. S.; Selinger, J. V.; Green, M. M. *Angew. Chem., Int. Ed.* **2000**, *39*, 1482−1485.

(14) Dekkers, H. P. J. M. In *Circular Dichroism*; Nakanishi, K., Berova, N., Woody, R. W., Eds.; VCH: New York, 1994; Chapter 6. The g_{abs} value is in general defined as $4 \cdot R/D$, where *R* and *D* are the rotatory and dipole strengths, respectively. A chiral polymer comprising a single helical state at a given condition should have the maximum g_{abs} value due to enantiopure helicity in analogy to determining the enantio-purity of chiral small molecules.

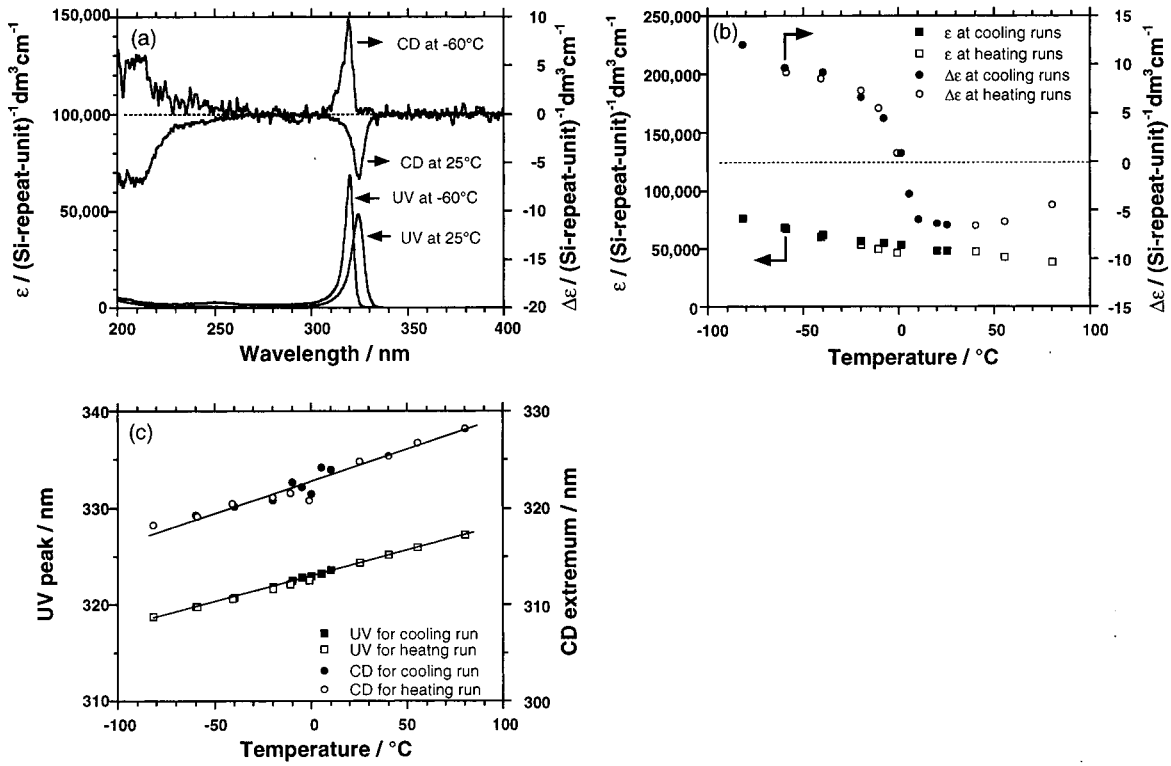

Figure 1. For **PS-1** in isooctane, (a) CD and UV absorption spectra at −60 °C and +25 °C, (b) variable temperature UV (squares) and CD (circles) intensities for cooling and heating runs, (c) variable temperature UV λ_{ext} (squares) and CD λ_{ext} (circles) wavelengths for cooling and heating runs.

through zero around 2 °C, and finally goes up to +11.8 at −80 °C. The compensation temperature (T_c), at which $\Delta\epsilon = 0$ (at 2 °C for **PS-1** in isooctane), is a result of the mutual cancellation of positive- and negative-CD signals due to the equal population of *P*- and *M*-motifs with the same photoexcited energy. The UV peak and CD extremum wavelengths of **PS-1** against temperature, however, are almost linearly blueshifted with lowering temperatures, as plotted in Figure 1c. The blueshift may be ascribed to a decrease in screw-pitch, deviating from an ideal 7_3-helical structure.[10d,11a]

Thus, **PS-1** can switch dynamically between *P*- and *M*-motifs at these temperatures. The CD signal was found to follow quickly the change in the solution temperature,[15] even in a fast heating run from −10 to 25 °C in less than 35 s, suggesting the occurrence of rapid helical inversion near T_c, on a time scale of less than 1 s.

Differing from **PS-1**, the positive-signed CD spectrum of **PS-2** with an extremum of 320 nm at −74 °C retains the positive Cotton effect with an extremum of 328 nm at +80 °C, as shown in Figure 2a. Also, from Figure 2b, the $\Delta\epsilon$ value monotonically changes from +4.7 at +80 °C to +13.3 at −83 °C, indicating no inversion of preferential screw-sense in this temperature range, though the CD spectra are consistent with their corresponding UV absorption profiles in the range of −83 to +80 °C.[15] This conclusion is also supported by the UV peak and CD extremum wavelength data shown in Figure 2c, which shows monotonic blueshifts for UV and CD with lowering temperature. However, it is not conclusive if **PS-2** undergoes a chiroptical inversion outside the temperature range investigated, since a measurement was impossible due to the freezing (−100 °C) and boiling (+100 °C) for isooctane.

As seen in Figures 1b and 2b, the UV peak intensities of **PS-1** and **PS-2** almost linearly increase with lowering temperature, ranging from ca. 40 000 at +80 °C to ca. 80 000 at −80 °C for **PS-1**, and from ca. 38 000 at +80 °C to ca. 75 000 at −83 °C for **PS-2**. These high ϵ values are due to their rodlike conformations of **PS-1** and **PS-2** over this temperature range, which have been established by viscometric and atomic force microscopy measurements.[10a−f] Indeed an almost linear increase in the ϵ value with decrease in temperature is in parallel with a progressive increase in the radius of gyration or end-to-end distance of the polysilylene.[10d]

It is an open question as to why **PS-1** undergoes such a steep chiroptical switching response to change in solution temperature. The answer may lie in the presence of quantized double well local free-energy minimum potentials of the dihedral angle,[9] leading to the coexistence of *P*- and *M*-motifs in the same silicon chain at all temperatures, even very low and high.

Figure 3, a and b, shows the Si−Si−Si−Si dihedral angle dependence of the potential energy of (*R*)-3,7-dimethyloctyl-(*S*)-3-methylpentyloligosilylene with 31 repeating units terminated with hydrogen (**oligo-PS-1**) and (*S*)-3,7-dimethyloctyl-(*S*)-3-methylpentyloligosilylene 31 repeating units terminated with hydrogen (**oligo-PS-2**) for their isotactic and syndiotactic stereoisomers, respectively. For these calculations, standard parameters with a Si−Si bond length of 2.34 Å and a Si−Si−Si bond angle of 111°, and the pcff force field (Molecular Simulation Inc., the Discover 3 module, Ver. 4.00) were used. Details are given in the Experimental Section.

Both **oligo-PS-1** and **oligo-PS-2** clearly indicate double-well potential curves which mean two local energy minima corresponding to almost enantiomeric helices with dihedral angles of about 150−160° (*P*-helix) and 200−210° (*M*-helix), regardless of their tacticity. The global minimum *P*-motif seems to be more stable than the corresponding *M*-motif. Since both **PS-1** and **PS-2** exhibit positive CD signals at lower temperatures, helical poly(dialkylsilylene)s adopting a preferential *P*-motif are assumed to result in positive CD signal, or vice versa. The relationship between helicity and the CD sign would be

(15) See Supporting Information.

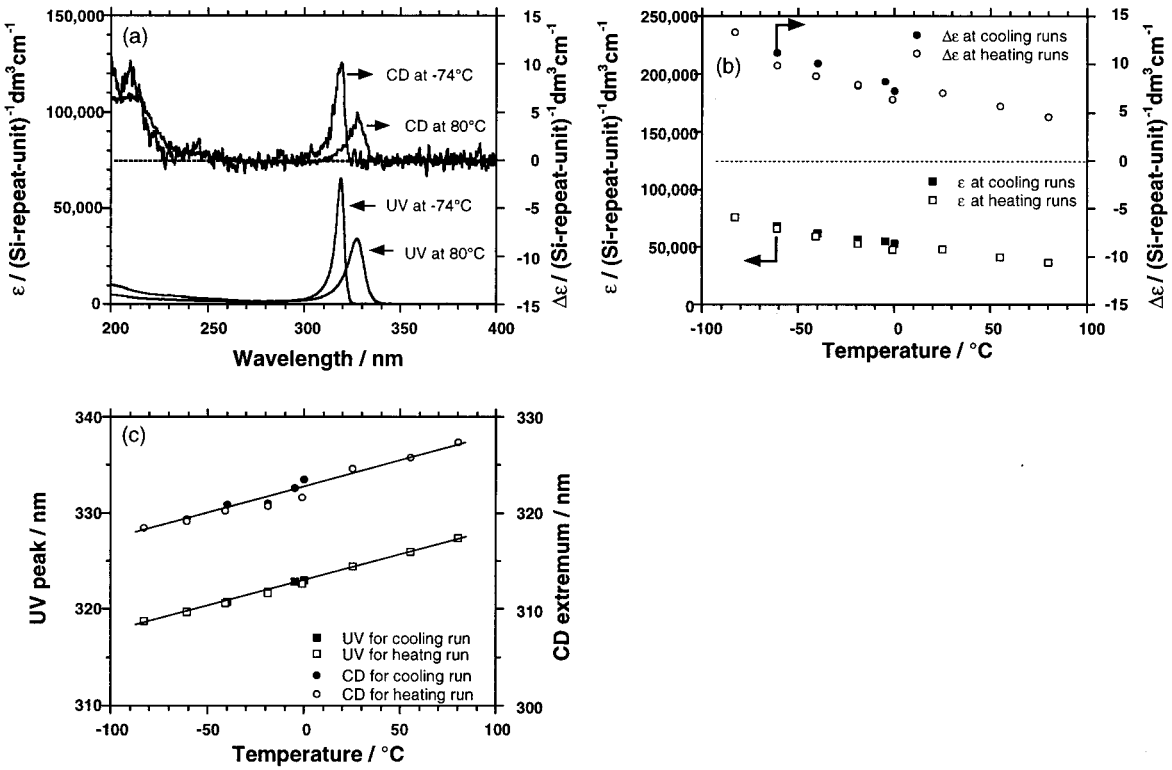

Figure 2. For **PS-2** in isooctane, (a) CD and UV absorption spectra at −74 °C and +80 °C, (b) variable temperature UV (squares) and CD (circles) intensities for cooling and heating runs, (c) variable temperature UV λ_{ext} (squares) and CD λ_{ext} (circles) wavelengths for cooling and heating runs.

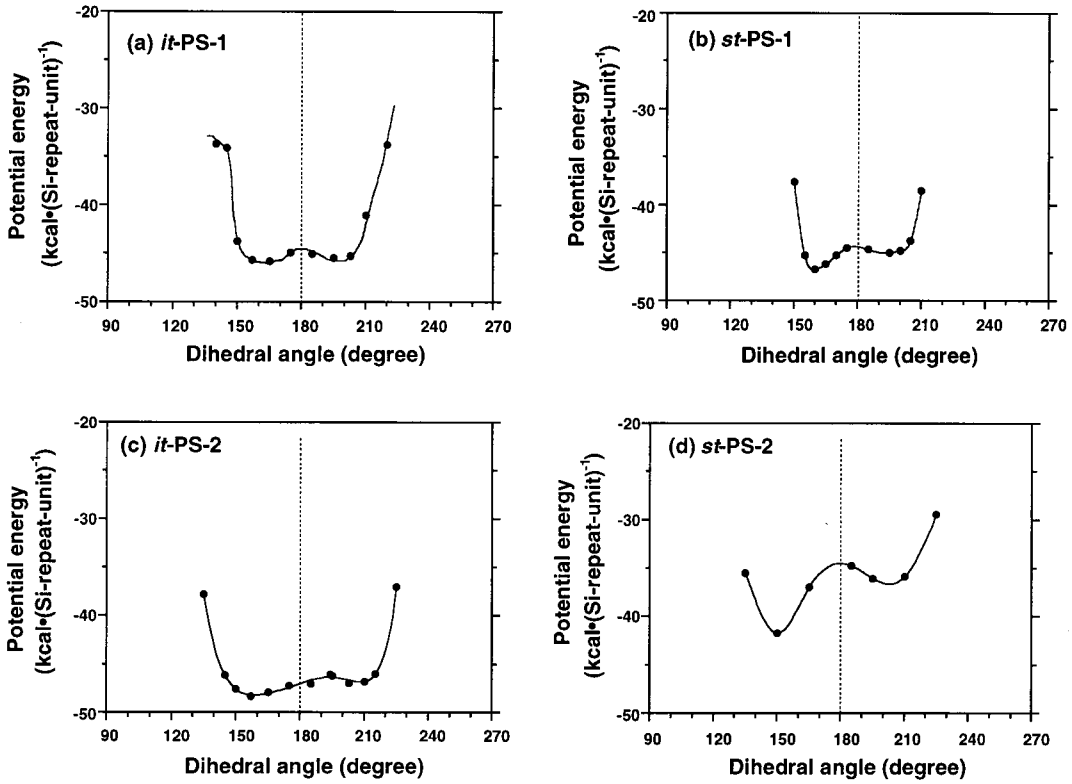

Figure 3. Dihedral angle dependence of the potential energy for **PS-1** or **PS-2** model molecules with 31 repeating units and hydrogen termini (**oligo-PS-1** or **oligo-PS-2**). For **oligo-PS-1**, (a) *isotactic* (*it*) sequences and (b) *syndiotactic* (*st*) sequences, and for **oligo-PS-1**, (c) *it* sequences and (d) *st* sequences.

consistent with that of a recently reported poly{(*S*)-3,7-dimethyloctyl-3-methyl-butylsilylene} (**PS-3**, Scheme 1) exhibiting inversion of preferential helicity at −20 °C.[11a]

In *it*-**oligo-PS-1**, the *P*-motif is more stable than *M*-motif by only 0.4 kcal·(Si-repeat-unit)$^{-1}$, while, in *st*-**oligo-PS-1**, *M* is more stable than *P* by 1.8 kcal·(Si-repeat-unit)$^{-1}$ (Figure 3, a and b). For *it*-**oligo-PS-2**, *M* is more stable than *P* by 1.5 kcal·(Si-repeat-unit)$^{-1}$, while *M* is greatly more stable than *P* by 5.2 kcal·(Si-repeat-unit)$^{-1}$ for *st*-**oligo-PS-2** (Figure 3, c and d).The other important feature may be the ratio of energy barrier heights

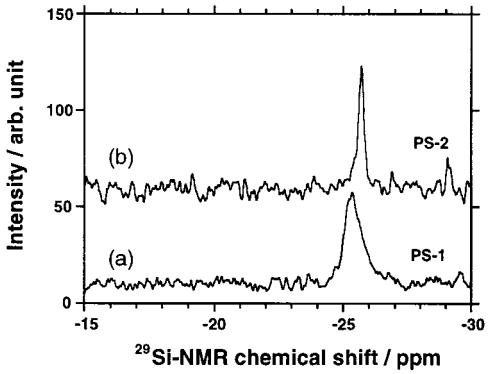

Figure 4. ^{29}Si NMR spectra of (bottom, a) **PS-1** (low-molecular weight fraction) and (top, b) **PS-2** (low-molecular weight fraction) in $CDCl_3$ at 20 °C.

between two minima at *P* or *M* and a hill existing at around 180° of dihedral angle.[11a] The role of conversion from one motif to another will be determined by the forward and backward barrier height energies. The barrier height ratios of *it*- and *st*-**oligo-PS-1**s are only about 1.6 and 3.6, respectively, whereas those of *it*- and *st*-**oligo-PS-2**s are fairly large, being about 4.1 and 3.4, respectively. This lower barrier height ratio of *it*-**oligo-PS-1** may lead to a rapid exchange between *P*- and *M*-twists, and be responsible for switching of the preferential screw-sense of actual **PS-1** without thermal hysteresis.[11a]

To discuss the screw-sense switching, we try to simply evaluate the energy parameters for the *P*- and *M*-motifs of **oligo-PS-1** and **oligo-PS-2**, in analogy with **oligo-PS-3**.[11a] Here, the ΔG is the difference in the Gibbs free energy between *P* and *M* screw senses, and the enthalpy (ΔH) and entropy (ΔS) terms are the differences in enthalpy and entropy between the *P* and *M* turns, respectively. Here, our calculation results of the oligomer models with sufficiently long repeating units would be applicable to the real polysilylenes, since these parameters are normalized as Si repeating unit. Thus we have

$$\Delta G = G_{\mathrm{P}} - G_{\mathrm{M}} = \Delta H - T\Delta S = H_{\mathrm{P}} - H_{\mathrm{M}} - T\,(S_{\mathrm{P}} - \mathrm{S_M}) \quad (1)$$

At the inversion temperature T_c, the enthalpy and entropy terms are just in balance to guide $\Delta G = 0$.[11a,11b] Therefore,

$$T_c = \Delta H/\Delta S \quad (2)$$

On the assumption that the value of ΔH is equal to the above calculated energy difference between *P*- and *M*-motifs and T_c = 275 K, we obtain $\Delta S = -1.5$ cal·(Si-repeat-unit·K)$^{-1}$ and $\Delta H/RT_c = -0.74$ at 275 K for *it*-**oligo-PS-1** and $\Delta S = -6.6$ cal·(Si-repeat-unit·K)$^{-1}$ and $\Delta H/RT_c = -3.3$ at 275 K for *st*-**oligo-PS-1**. The absolute magnitude of $\Delta H/RT_c$ for the *it* is almost identical to that of **PS-3** with 1.0,[10] whereas that for the *st* is fairly large. Below T_c, ΔG is negative, and the *P*-motif is more stable than the *M*-motif, which is reversed above T_c. The inversion of ΔG term is caused by TΔS term, which is therefore responsible for the switching of preferential helical screw-sense.

Noticeable differences among **PS-1**, **PS-2**, **PS-3**, and **PS-4** are their signal line widths ($\Delta\nu_{1/2}$) and chemical shifts in ^{29}Si NMR in $CDCl_3$ at 20 °C, as displayed in Figure 4. The line width and chemical shifts are closely related to the degrees of main chain rigidity and mobility of polysilylenes.[10a,11a] The greater degree of flexibility of **PS-2** compared to **PS-1**, **PS-3**, and **PS-4** is suggested by the narrower $\Delta\nu_{1/2}$: for **PS-2**, $\Delta\nu_{1/2}$ = ca. 14 Hz at −25.7 ppm; for **PS-1**, $\Delta\nu_{1/2}$ = 46 Hz at −25.3 ppm; for **PS-3**,[11a] $\Delta\nu_{1/2}$ = 29 Hz at −25.3 ppm; and for **PS-4**,[11a] $\Delta\nu_{1/2}$ = 65 Hz at −22.7 ppm. However, the chemical shift of **PS-1**, **PS-2**, and **PS-3** are upfield compared to that of **PS-4** by ca. 2.5−3.0 ppm. The downfield chemical shift of **PS-4** is considered to originate from elongation of the Si−Si bond length resulting from the steric demand by fixing hindered β-branched alkyl side chains.[10a] This is because the chemical shifts of flexible rodlike helical **PS-1**, **PS-2**, and **PS-3** with less sterically hindered γ-branched alkyl side chains[10a,11] are very close to that of greater flexibile poly(di-*n*-hexylsilane) in the disordered solid phase.[12] These observations infer that helical polysilylenes able to switch the preferential screw sense may commonly have $\Delta\nu_{1/2}$ of 30−50 Hz at around −25 ppm in ^{29}Si NMR spectrum at ambient temperature.

2.2. Quantized and Superposed Helicities. The variable temperature g_{abs} values of **PS-1**, **PS-2**, and **PS-4** in isooctane are plotted in the range from −80 to +80 °C (Figure 5a). The slight temperature dependence of the g_{abs} values even in **PS-4** is due to a decrease of screw-pitch, as indicated by the progressive blueshift of the UV λ_{max} with decrease in temperature.[10d,11a,16] Here we assume that **PS-4** includes purely *P*-motif over the temperature range studied and use its g_{abs} value, $g_{max}^{P}(T)$, to re-normalize the g_{abs} values for **PS-1** and **PS-2** at each temperature such that

$$P(\%) = 100[1 + g_{abs}(T)/g_{max}^{P}(\mathrm{T})]/2 \quad (3)$$

$$M(\%) = 100 - P\,(\%) \quad (4)$$

where *P*(%) and *M*(%) are the mol % of the *P*- and *M*-motifs, respectively, and $g_{abs}(T)$ is the observed g_{abs} at *T*. From the second-order regression curve of $g_{max}^{P}(T)$ for **PS-4**, we obtain

$$g_{max}^{P}(\mathrm{T}) = 2.29 - 3.22 \times 10^{-3}\cdot T - 1.72 \times 10^{-6}\cdot T^2 \quad (5)$$

where *T* is in °C and g_{abs} is in 10^{-4} unit.

It should be noted that **PS-1** features three key, thermally accessible regions, 1 (−80 to −10 °C), 2 (−10 to +10 °C), and 3 (+10 to +80 °C), as indicated in Figure 5b. In region 1, **PS-1** contains a constant 20% *P* and 80% *M* (60% *M* excess), but contrarily in region 3, it has 80% *P* and 20% *M* (60% *P*-excess). However, **PS-2** invariably contains 20% *P* and 80% *M* (60% *M*-excess) over the entire temperature range (−80 to +80 °C). This leads to the idea that the seesaw-like switching of states between regions 1 and 3 may be quantized as the stationary state of *P*- and *M*-superposition, but not due to 100% pure *P*- and *M*-states. These estimates are derived from the above assumption about *P*(%), whose accuracy is needed to check by other means for a more quantitative discussion.

To explain this unique variable temperature helical state, it might be necessary to assume that cooperativity in coupled electronic and conformational transitions is related to the origin of the steplike switching response to the thermal energy bias. The effect of the electronic coupling has been theoretically discussed for π-conjugating polyenes with conformational defects,[17] and the conformational effect has already been established for electronically nonconjugating stiff helical polyisocyanate systems.[13]

Since the values of ϵ and λ_{max} around T_c change almost linearly with the variation of the solution temperature (Figure 1, b and c), it is possible that, in an electronically conjugating, stiff helical polysilylene with discrete energy levels[10g] in a double-well potential, the wave function of the lowest ground-

(16) Teramae, H.; Takeda, K. *J. Am. Chem. Soc.* **1989**, *111*, 1281−1285.
(17) (a) Stratt, R. M.; Smithline, S. J. *J. Chem. Phys.* **1983**,*79*, 3928−3937. (b) Schweizer, K. S. *J. Chem. Phys.* **1986**, *85*, 4181−4193.

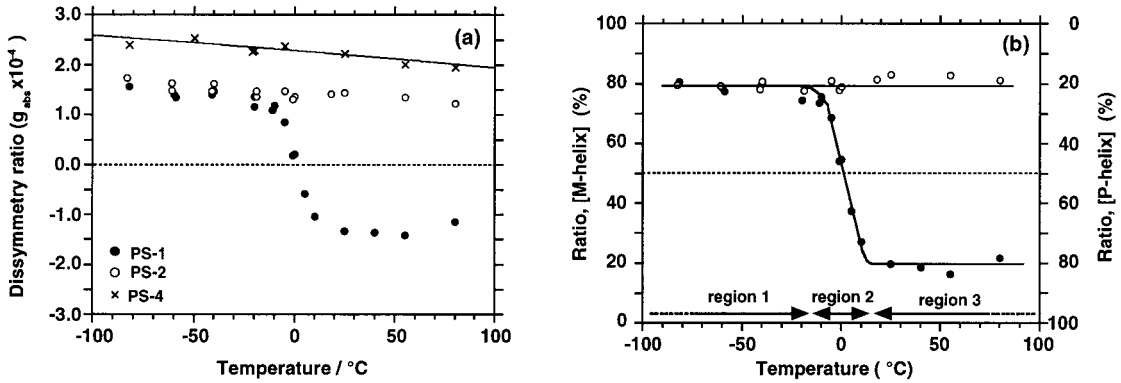

Figure 5. (a) Variable temperature g_{abs} values of **PS-1** (high-molecular weight fraction, filled circles), **PS-2** (high-molecular weight fraction, open circles), and **PS-4** (filled squares) in isooctane in the range of −80 and +80 °C. (b) *P*−*M* fraction of **PS-1** (filled circles) and **PS-2** (open circles) as a function of temperature.

state at an *M*-state electronically communicates with that of a *P*-state through quantum mechanical tunneling between the *P*- and *M*-electronic states. Although the situation has already been discussed theoretically for wave functions of hypothetical chiral molecules,[9] it is necessary to invoke the presence of helix reversals in the case of helical polymers.[13,17] The helix reversal, probably consisting of several silicon−silicon single bonds (0.2−1.0 nm in length) is the section in which the screw-sense changes direction, and might act as a moderately small tunneling barrier. The reversal may play a crucial role in correcting errors from thermal noise through dynamic winding and rewinding motions from one screw-sense to the other. The helix reversal may exist as very short all-anti, transoid, or $TG^{+}TG^{-}$ sequence.[18] For the purpose of presentation, the idea was schematically illustrated in Supporting Information,[15] where a helix reversal was expressed by a triad "bit −1 bit +1 bit −1" or "bit +1 bit −1 bit +1" and a helical sequence by a consecutive bit −1's or bit +1's. Since the chain conformation is expected to change as such a triad moves along the chain, the direct molecular imaging and spectroscopic identification of the helix reversal as well as structural analysis of the dynamic motion are currently ongoing.

Apparent time-averaged optical inactivity at T_c may result from a rapid interconversion between *P* and *M* (oscillating helicity or dynamic pseudoracemization). In this quasi-stationary state, the wave functions of the superposed *P*- and *M*-states (P_s- and M_s-states) may produce two splitting sublevels, $\Psi = 1/\sqrt{2}$-$[\Psi_{Ps} \pm i\Psi_{Ms}]$.[9] This is a result of electronic coupling between the lowest energy levels of *P*- and *M*-helical states, which are almost degenerate, confined in the same one-dimensional helical silicon semiconducting wire.[10g,11a] These helical exciton absorptions are unique because of negligible weak electron−phonon coupling,[10g] a feature not seen in π-conjugating polymers or small molecules. Actually, vibronic phonon-side bands in the high energy region of the near-UV band at 320 nm are just discernible in Figures 1 and 2. Two hypothetical energy models with two splitting sublevels are illustrated in Figure 6.

In region 1 below T_c, the higher level in the *P*-state mainly interacts with the lower level in the *M*-state, whereas in region 3 above T_c, the lower level in the *P*-state interacts with the higher level in the *M*-state. If these interactions are reasonably strong, both the *P*- and *M*-state populations may be significant and rather insensitive to temperature change. On the other hand, in region 2 encompassing T_c, higher and lower levels in the *P*-state

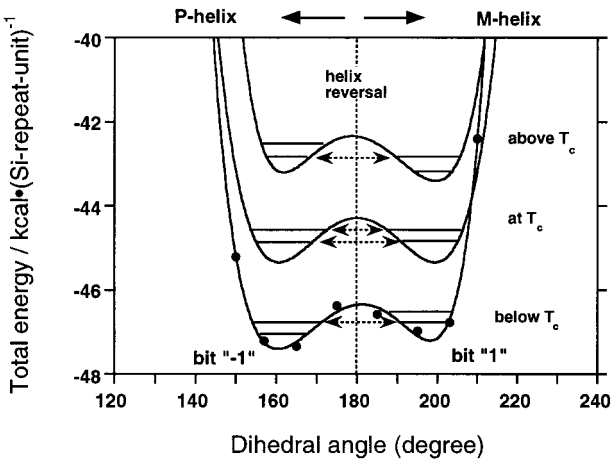

Figure 6. Potential energy as a function of main chain dihedral angles with three switching regions. Below T_c (bottom trace with circles calculated at zero Kelvin), at T_c (middle trace, hypothetical curve), and above T_c (upper trace, hypothetical curve). Dotted arrows indicate tunneling processes between wave functions of *P*- and *M*-motifs existing in the same backbone.

interact with the higher and lower levels in the *M*-state each other. Assuming that $\Delta E_{PM} \approx 20$ K or 1.1×10^{-3} eV (transition width in region 2 for superposed *P* and *M*), one may suppose a racemization time (T_{rac}) of 2.7×10^{-12} sec, corresponding to oscillating helicity (δ) of ca. 13 cm^{-1} from the time−energy uncertainty principle ($\Delta E \Delta T \geq h$).[9] The direct detection of the tiny splitting levels or oscillation frequency may be in the realm of high-resolution vibration in far-infrared region, fluorescence, and UV spectroscopy,[9,19] although Si−Si vibrations are observed in the range of 450−550 cm^{-1}. The expected oscillation frequency may be the almost similar magnitude of the proton tunneling splitting energy for tropolone derivatives in a supersonic free jet, determined by fluorescence spectroscopy.[19]

More detailed dimensional characterization including chiroptical analysis as functions of molecular weight and temperature will provide more realistic molecular and energetic parameters of **PS-1** and **PS-2**, such as the energy costs of the helix reversal (ΔG_r) and preferential helix induction (ΔG_h), persistence length (q), and lower-molecular weight limit of switching properties.[13] Preliminary investigation of low-molecular weight **PS-1** (Si repeating number is approximately 290) revealed that the *P*- and *M*-ratios in regions 1 and 3 and the T_c

(18) (a) Zink, R.; Magnera, T. F.; Michl J. *J. Phys. Chem. A* **2000**, *104*, 3829−3841. (b) Ottosson C−H.; Michl J. *J. Phys. Chem. A* **2000**, *104*, 3367−3380.

(19) Sekiya, H.; Tsuji, T.; Ito, S.; Mori, A.; Takeshita, H.; Nishimura, Y. *J. Chem. Phys.* **1994**, *101*, 3464−3471.

value are almost identical to those of the high-molecular weight fraction, except that the transition width in region 2 is slightly broadened.[15] This suggests that even such a lower M_w **PS-1** can effectively switch a preferential screw-sense in response to change in temperature.

A recent theory and analysis for "temperature effect" of optically active polyisocyanate terpolymers able to alter a preferential screw-sense[13e] could be applicable to an advanced discussion for **PS-1**. Detailed characterization of those ΔG_r, ΔG_h, and q parameters based on quantitative analysis on molecular weight and temperature dependence of chiroptical, light scattering, and viscometric data is now ongoing using the current theories for wormlike chain.[20]

Interest in the superposition of bi-stable quantum states at low temperature is now growing in the area of the quantum computing.[8] The apparent superposition of **PS-1** results from time averaged *M*- and *P*-states at almost ambient temperature. This may lead to the idea that the helical superposition could be achievable even in a single molecule. If we assume for a chainlike 70-mer that the 10 7_3 helical unit cell corresponds to a bi-stable bit responsive to thermal and chemical sources, a single helical polysilylene molecule with 70 Si−Si bonds, corresponding to 10 qubits, may be able in principle, therefore, to process huge amounts of chemical information, reaching 2^{10}. Alternatively, if fine temperature resolution of 0.1 K is practicably attainable, a transition temperature of 20 K in region 2 might possibly permit the recognition of ca. 200 different molecular shapes. Although direct detection of oscillating helicity might be the next challenge, our understanding and insight of the quantized and superposed helicities masking the switchable optically activity of conjugating polymers may lead to the more realistic design of a molecular information processor linked to the dynamic twisting molecular motion. As a preliminary test of this idea, we investigated the solvent molecule recognition ability of **PS-1**, as described in section 2.3.

2.3. Molecular Shape Recognition by Superposed Switching and Dynamic Memory. The most important feature of **PS-1** exists in region 2, because the superposed state linearly varies with thermal energy bias, ranging from 60% *M* to 60% *P* excess. It is noted that **PS-1** sensitively recognizes the topology of small molecules[21] due to the three-branched structures of the two chiral pendants. In other words, the superposed states linked by dynamic twisting motions may also be considered to comprise a "dynamic memory" function, since if the solvent molecules (external chemical bias) are taken away, the superposed state may result in modifying the *P*−*M* population of **PS-1**. This may be proved by a change in T_c value with a range of nonpolar hydrocarbon solvent molecules with different degrees of branching. This may be called as "solvent effect" of optically active polymers able to alter a preferential screw-sense, as demonstrated in optical activity of poly(*n*-hexylisocyanate) induced by enantiopure chiral, racemic, and achiral solvents.[13c] The energetic analysis for this may be applicable to the present **PS-1** systems, similar to the temperature effect mentioned above.

Figure 7 compares the variable temperature *P*−*M* population of **PS-1** (low-molecular weight fraction) in three typical solvents with different degree of branching, including *n*-heptane (linear hydrocarbon), methylcyclohexane (cyclic hydrocarbon), and 2,2,4,4,6,8,8-heptamethylnonane (highly branched hydrocarbon).

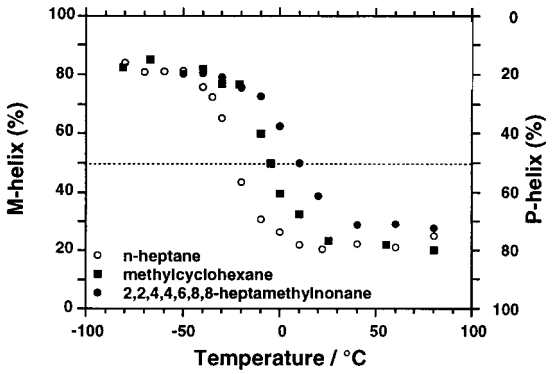

Figure 7. Variable temperature *P*−*M* fraction of **PS-1** (low-molecular weight fraction) in 2,2,4,4,6,8,8-heptamethylnonane (filled circles), methylcyclohexane (filled squares), and *n*-heptane (open circles) in the range of −80 and +80 °C.

Table 1. Solvent Molecular Topology Effect of the T_c Value in **PS-1**

Solvent	Chemical structure	T_c /°C	No. of branches based on C5 chain	Balaban index
2,2,4,4,6,8,8-Heptamethylnonane	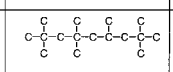	10	4.5	94
Isooctane (2,4,4-Trimethylpentane)	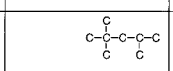	2	3	30
2,3,4-Trimethylpentane	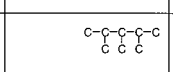	0	3	30
Methylcyclohexane	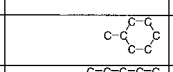	-5	2	18
3-Methylpentane	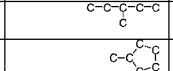	-14	1	14
Methylcyclopentane	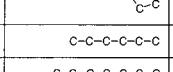	-14	1	17
n-Hexane	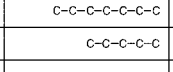	-20	0	12
n-Heptane	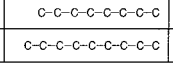	-23	0	13
n-Pentane		-25	0	9
n-Octane	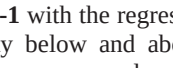	-25	0	16
n-Nonane	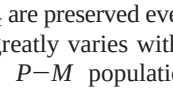	-25	0	17

The population was evaluated from the variable temperature g_{abs} values of **PS-1** with the regression g_{abs} curve of **PS-4**. The quantized helicity below and above T_c, and the superposed helicity around T_c are preserved even in these solvents. Although the value of T_c greatly varies with the degree of branching of the solvent, the *P*−*M* population below T_c seems to be insensitive to the degree of branching but above T_c, to be very sensitive.

The effects of solvent topology on T_c for various solvents are summarized in Table 1, where the degree of branching is defined as the Balaban index number[21] and numbers of branching carbons per linear five-carbon sequence. Considering in intrusion of branched solvent molecules into the branched side chains in the ordered state of **PS-1** in an ordered state below T_c, which may lead to an unfavorable packing of pendants,[11a] this results in an increase of S_p but no change of S_M in eq 1. This means a decrease in the ΔS term and an increase in T_c, since the entropy term is responsible for determining T_c.

The degree of the interaction might be greatly affected by the degree of solvent branching. As seen in Table 1, straight chain alkyl molecules give a lower T_c, whereas branched chain alkyl molecules tend to afford a higher T_c and branched cyclic solvents give an intermediate value. Quantitatively, it is shown

(20) (a) Yamakawa, H. *Helical Wormlike Chains in Polymer Solutions*; Springer: Berlin, 1997. (b) Kratky, O.; Porod, G. *Recl. Trav. Chim.* **1949**, *68*, 1106. (c) Norisuye, T.; Tsuboi, A.; Teramoto, A. *Polym. J.* **1996**, *28*, 357−361.

(21) Rouvray, D. H. *Sci. Am.* **1986**, *255(3)*, 36−43.

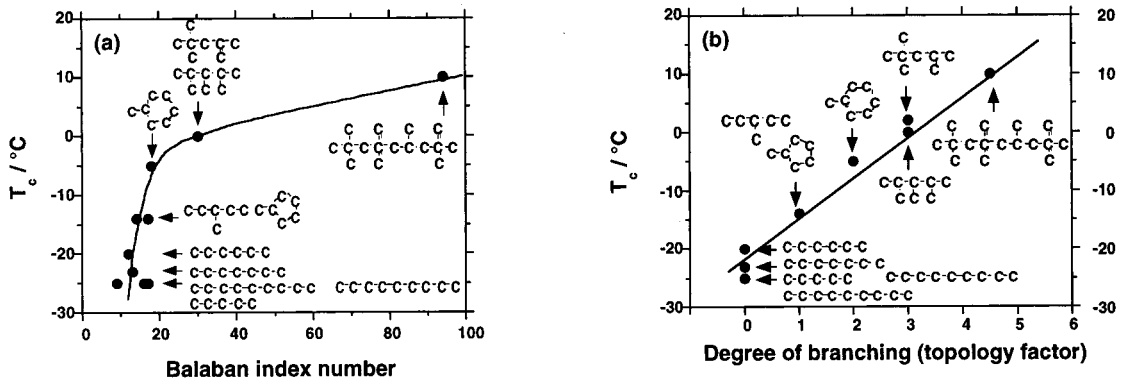

Figure 8. Change in the T_c value of **PS-1** (low-molecular weight) as a function of degree of branching in a range of hydrocarbon solvent molecules. The degree of branching is evaluated by (a) Balaban index number,[21] and by (b) number of branching points, compared to five linear carbon sequence since *(S)*-3-methylpentyl pendant is regarded to contain five carbon atoms and one branching carbon atom. In the case of cyclic hydrocarbons, we are regarded that methylcyclopentane consists of five carbon atoms of ring and one branched carbon and methylcyclohexane has five carbon atoms of ring and two branched carbons.

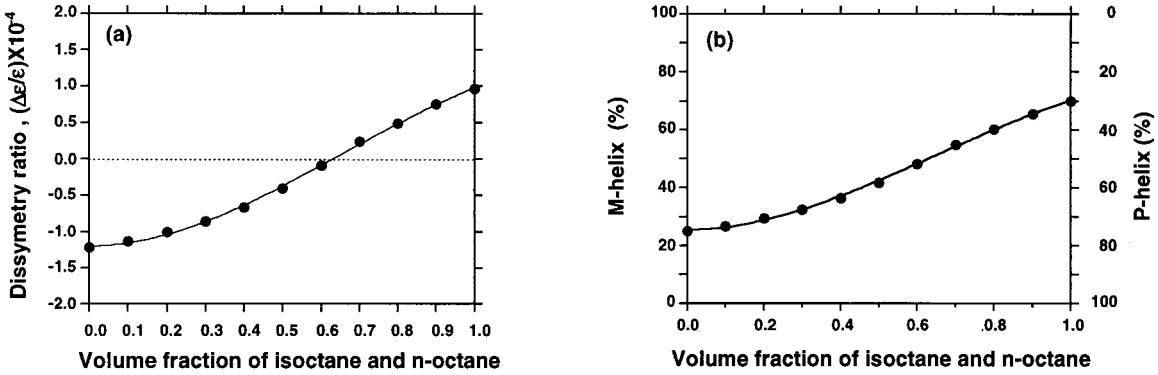

Figure 9. (a) Value of g_{abs} and (b) $P-M$ fraction of **PS-1** (low-molecular weight fraction) at −10 °C as a function of volume fraction of isooctane and *n*-octane.

in Figure 8, a and b, that T_c increases nonlinearly with increasing the Balaban index number, whereas T_c increases almost linearly with increasing the degree of branching of the solvent molecule defined here. The correlation of T_c to the Balaban index number is not as good as the degree of branching.

It was also found that the superposition states derived from the g_{abs} value and $P-M$ population of **PS-1** in the region 2 are very susceptible to the volume fraction of mixed isooctane and *n*-octane solvents at −10 °C (Figure 9, a and b). The superposed states give a slightly nonlinear response to the volume fraction of isooctane, indicating a weak cooperative interaction between the pendants and the solvent molecules.

These change in T_c with solvent topology and composition allows one to determine topology and composition of a wide range of molecules. This may lead to new method for tackling the current issue of predicting the chemical and biological properties of unknown chemicals from the molecular-connectivity index, which could help in modeling the toxicity and spread of pollutants, in developing anesthetics and psychoactive drugs, in predicting the degree of pollutants in the environments, in estimating the cancer-causing potential of chemicals, and in predicting the taste and smell of new substances.[21]

3. Conclusions

Electronically conjugating helical polymer, poly{(*R*)-3,7-dimethyloctyl-(*S*)-3-methylpentylsilylene} (**PS-1**) consisting of a rodlike silicon backbone and enantiopure chiral pendants, and its diastereomeric poly{(*S*)-3,7-dimethyloctyl-(*S*)-3-methylpentyl-silylene} (**PS-2**), were prepared. Molecular mechanics calculations of these oligomer models revealed double-well potential curves, showing two local steric energy minima corresponding to almost enantiomeric helices with dihedral angles of about 150−160° (*P*-helix, global minimum) and 200−210° (*M*-helix), regardless of their tacticity.

PS-1 in solution was found to exhibit switchable helicity with a "dynamic memory", that is susceptible to thermal energy bias and chemical environment. Although **PS-1** in isooctane features three distinct switching regions, "1, between −80 and −10 °C", "2, between −10 and +10 °C", and "3, between +10 °C and +80 °C", these switching properties were understood as a result of the superposition of P- and M-helicities, due to dynamic pseudoracemization or oscillating helicity.

Electronic coupling between the almost degenerate, lowest-energy levels of *P*- and *M*-helical motifs in the same main chain may give wave functions of the superposed *P*- and *M*-states with two splitting sublevels. In region 2, higher and lower levels in the *P*-state mutually interact with those in the *M*-state. We derived an oscillating helicity of about 13 cm^{-1}, corresponding to a racemization timeof 2.7×10^{-12} sec, from the time−energy uncertainty principle ($\Delta E \Delta T \geq h$) and $\Delta E_{PM} \approx 20$ K (1.1×10^{-3} eV). The superposed helicity in region 2 is critical, since it affords molecular recognition ability with a dynamic memory function which is highly susceptible to solvent molecular topology and mixed solvent volume fraction.

PS-2, however, did not switch preferential screw-sense in the range from −83 to +80 °C. This may be related to the fact that the backbone mobility of **PS-2** may be greater, as suggested from the narrower ^{29}Si NMR line widths, and greater differences in relative energy stability between *P* and *M*, and energy barrier heights in the potential energy.

4. Experimental Section

4.1. Measurements. CD and UV absorption spectra were recorded simultaneously on a *JASCO* J-720 spectropolarimeter equipped with a liquid nitrogen-controlled quartz cell with path length of 5 mm in a cryostat, ranging from 23 to −90 °C, and a Peltier-controlled quartz cell with path length of 10 mm, ranging from 80 to −10 °C. Detailed measurement conditions have already described in the literature.[11] The sample concentration was 2×10^{-5} (Si-repeat unit)$^{-1}$ dm^{-3} for UV and CD measurements. ^{13}C (75.43 MHz) and ^{29}Si (59.59 MHz) NMR spectra were taken in $CDCl_3$ at 30 °C with a Varian Unity 300 NMR spectrometer using tetramethylsilane as an internal standard. Optical rotation at the Na−D line was measured with a *JASCO* DIP-370 polarimeter using a quartz cell with path length of 10 mm at room temperature (24 °C). The weight-average molecular weight (M_w) and number-average molecular weight (M_n) of the polymers were evaluated using gel permeation chromatography (Shimadzu A10 instruments, Shodex KF806M as a column, and HPLC-grade tetrahydrofuran as eluent at 30 °C), based on a calibration with polystyrene standards.

The enantiopurity of starting materials and intermediates were determined at Toray Research Center (TRC, Shiga, Japan) using the chiral gas chromatography technique (Spelco, *β*-DEX-325 and *β*-DEX-225, 30 m × 0.25 mm ID, column oven temperature 70−95 °C, He carrier with 1.2 mL/min). Detailed analytical conditions were *β*-DEX-325 at 70 °C for **4** and **9**, *β*-DEX-225 at 82 °C for **6** and **10**, and *β*-DEX-225 at 90 °C for **7** and **11** (see in section 4.3.). We concluded that the enantiopurities of **4**, **6**, **7**, **9**, **10**, **11** used in this work were sufficiently high with almost identical ee's. However, the chiral GC analysis at the TRC indicated that the enantiopurity of (*S*)-(−)-*β*-3,7-citronellol (Merck, $[\alpha]^{24}_D = -3.11°$ (neat), corresponding to 68.4% ee based on $[\alpha]^{24}_D$ of purer **11** by Fluka) was only 64.8% ee, and also (*S*)-(−)-3,7-dimethyloctanol (Chemical Soft (Kyoto, Japan), based on the Merck product) was 66.4% ee. On the basis of the analysis, we used **7**(Fluka) and **11** (Fluka) only as starting materials.

4.2. Molecular Mechanics Calculations. Molecular mechanics calculation was performed using the Molecular Simulation Inc., the Discover 3 module, Ver. 4.00 on Silicon Graphics Indigo II XZ based on standard default parameters with a Si−Si bond length of 2.34 Å and a Si−Si−Si bond angle of 111° using the MSI pcff force field suitable for polymers. For this calculation, the MSI built-in function of simple-minimize (default: dihedral angle restraints, the steepest descents with the first derivative for 1.0, iteration limit 1000, movement limit 0.2, followed the conjugate gradients) and simple-dynamics (default: constant volume and constant temperature, initial temperature 300 K, time step 1 fs, velocity Verlet integration method, initial velocity is random from Boltzman distribution) were used.

Initially, after an oligomer model (31 repeating units terminated with hydrogen) with dihedral angle of 180° was generated, two oligomer models with dihedral angle of 150° and 210° were preliminarily generated. Next, calculation of *P*-screw-sense oligomer model setup with desired dihedral angle was carried out based on the 150°-model, and *M*-models were based on the 210°-model, respectively.

4.3. Monomer Preparation. The synthetic procedure for *(R)*-(+)-3,7-dimethyloctyl-*(S)*-3-methylpentyldichlorosilane (**1**) is described. *(S)*-3-Methylpentyltrichlorosilane (**2**) was obtained by coupling 68 g (0.40 mol) of tetrachlorosilane (Shin-Etsu) with the Grignard reagent formed from 29.5 g (0.25 mol) of *(S)*-(+)-3-methylpentyl chloride (**3**) (Chemical Soft). Colorless liquid. Yield 33.3 g (76%); bp 70−73°/6.5 mmHg, $[\alpha]^{24}_D = +2.25°$ (neat). ^{29}Si NMR ($CDCl_3$, 30 °C) 13.66 ppm, ^{13}C NMR ($CDCl_3$, 30 °C, ppm) 19.00, 21.66, 22.61, 22.70, 24.67, 27.95, 28.93, 34.38, 36.39, 39.24. Dichlorosilane **1** was obtained by slowly adding Grignard reagent (**5**) obtained from 33 g (0.15 mol) of (*R*)-(−)-3,7-dimethyloctylbromide (**4**, $[\alpha]^{24}_D = -5.96°$ (neat), 96.6% ee) to 17.4 g (79 mmol) of **2** in dry diethyl ether at room temperature. The bromide **4** was prepared at Chemical Soft by bromination of (*R*)-(+)-3,7-dimethyloctanol (**6**, $[\alpha]^{24}_D = +3.90°$ (neat), 95.7% ee) with PPh_3 and Br_2 in CCl_4, followed by hydrogenation of (*R*)-(+)-*β*-citronellol (**7**) (Fluka, $[\alpha]^{24}_D = +4.46°$ (neat), 97.4% ee).

Filtration of the reaction mixture and vacuum distillation of the filtrate afforded pure **1**. Colorless liquid. Yield 9.8 g (42%); bp 108−113°/0.20 mmHg, $[\alpha]^{24}_D = +3.18°$ (neat). ^{29}Si NMR ($CDCl_3$, 30 °C, ppm) 34.73, ^{13}C NMR ($CDCl_3$, 30 °C, ppm) 11.33, 17.38, 18.64, 22.63, 22.72, 24.76, 27.99, 28.70, 28.73, 29.14, 34.81, 36.44, 36.48, 39.32.

(*S*)-(+)-3,7-Dimethyloctyl-(*S*)-3-methylpentyldichlorosilane (**8**) was synthesized in a similar way using (*S*)-3,7-dimethyloctylbromide (**9**, $[\alpha]^{24}_D = +6.05°$ (neat), 95.0% ee) (Chemical Soft) from (*S*)-(−)-3,7-dimethyloctanol (**10**, $[\alpha]^{24}_D = -4.22°$ (neat), 95.9% ee) and (*S*)-(−)-*β*-citronellol (**11**, Fluka, $[\alpha]^{24}_D = -4.55°$ (neat), 97.4% ee) as starting material. Colorless liquid; bp 109−113°/0.20 mmHg, $[\alpha]^{24}_D = +5.60°$ (neat). ^{29}Si NMR ($CDCl_3$, 30 °C, ppm) 34.75, ^{13}C NMR ($CDCl_3$, 30 °C, ppm) 11.32, 17.37, 18.64, 19.11, 22.63, 22.71, 24.75, 27.98, 28.70, 29.14, 34.80, 36.44, 36.47, 39.31.

4.4. Polymer Preparation. A typical synthetic procedure is described as follows for **PS-1**. To a mixture of 12 mL of dry toluene (Kanto), 0.50 g (22 mmol) of sodium (Wako), and 0.06 g (0.23 mmol) of 18-crown-6 (Wako), 1.6 g (4.9 mmol) of **1** was added dropwise in an argon atmosphere. The mixture was stirred slowly at 110 °C. After 2 h, 150 mL of dry toluene was added to reduce solution viscosity and stirring was continued for a further 30 min. The hot reaction mixture slurry was passed immediately through a 5-*μ*m PTFE filter under argon gas pressure. To the clear filtrate, 2-propanol and ethanol as precipitating solvents were added carefully. Several portions of white precipitates were collected by centrifugation and dried at 120 °C under vacuum overnight.

For **PS-1**, high-molecular weight (HMW) fraction: $M_w = 5.83 \times 10^6$ (DP_w = ca. 23 000) and $M_n = 3.44 \times 10^6$; low-molecular weight (LMW) fraction: $M_w = 7.36 \times 10^4$ (DP_w = ca. 290) and $M_n = 2.47 \times 10^4$; for **PS-2**, HMW fraction, $M_w = 4.67 \times 10^6$ (DP_w = ca. 18 400) and $M_n = 2.09 \times 10^6$, LMW fraction, $M_w = 6.37 \times 10^4$ (DP_w = ca. 250) and M_n = 23400. ^{29}Si NMR ($CDCl_3$, 20 °C, ppm); for **PS-1** (LMW fraction): −25.32; for **PS-2** (LMW fraction): −25.69, ^{13}C NMR ($CDCl_3$, 20 °C, ppm, major peaks); for **PS-1** (LMW fraction):11.95, 17.38, 18.77, 22.57, 22.75, 25.58, 28.11, 28.70, 28.73, 29.14, 34.81, 36.86, 36.48, 39.39; for **PS-2** (LMW fraction, major peaks): 11.91,19.00, 22.56, 22.74, 25.58, 28.13, 29.06, 35.34, 37.18, 38.51, 39.36.

Acknowledgment. We thank Hiromi Tamoto-Takigawa for preliminary CD and UV measurements. Drs. Masao Morita, Keiichi Torimitsu, and Hideaki Takayanagi are gratefully acknowledged for their continuing support. Professors Takahiro Sato, Junji Watanabe, Masashi Kunitake, Shoji Furukawa, and Eiji Yashima are acknowledged for fruitful comments and discussion. Drs. Zhong-Biao Zhang and Hongzhi Tang are acknowledged for discussion. Correspondence and requests for material and Supporting Information should be addressed to M.F. (e-mail: fujiki@will.brl.ntt.co.jp).

Supporting Information Available: Variable temperature UV and CD spectra of **PS-1** (HMW fraction) in isooctane at −80, −40, −20, −10, −8, −5, 0, 5, 10, 25, 55, and 80 °C, variable temperature UV and CD spectra of **PS-2** (HMW fraction) in isooctane at −83, −61, −40, −19, −5, 0, 25, 55, and 80 °C, variable temperature g_{abs} values of **PS-1** (HMW and LMW fractions) and **PS-2** (HMW fraction), which are normalized by the regression g_{abs} curve of **PS-4**, and schematic illustration of twisting and translational motions of helical motifs and helix reversals (PDF). This material is available free of charge via the Internet at http://pubs.acs.org.

JA0026509